Diamantane molecules ...

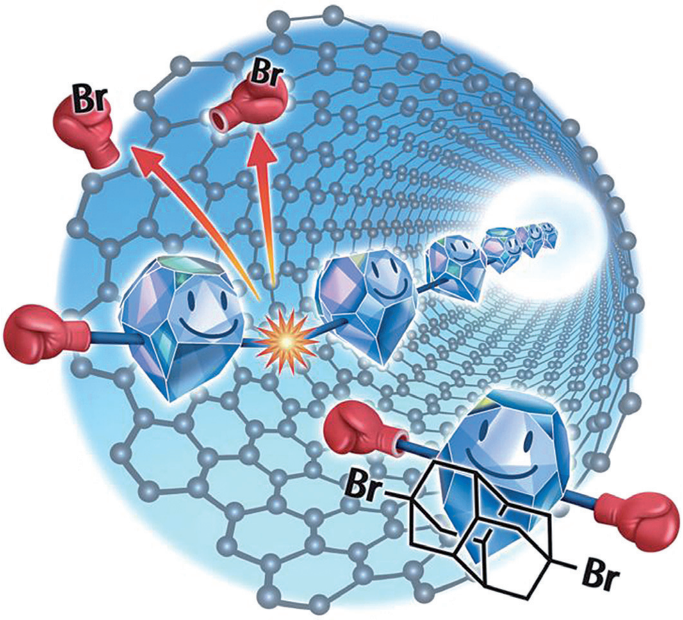

... form perfect linear-chain nanowires inside double-walled carbon nanotubes. In their Communication on page 10802 ff., H. Shinohara and co-workers describe how these nanowires are synthesized in a template reaction of dibrominated diamantane precursors in the hollow cavities of the carbon nanotubes. Under high vacuum and in the presence of iron nanocatalyst particles, the dehalogenated radical intermediates spontaneously form linear polymer chains within the nanotubes.

Hydrogen Evolution

In their Communication on page 10751 ff., T. Asefa, W. Chen, X. Zou, et al. report an efficient hybrid hydrogen-evolution electrocatalyst consisting of molybdenum carbide nanoparticles embedded in nitrogen-rich carbon nanolayers. The synergistic effect between Mo_2C and N dopants co-activates adjacent C atoms on the carbon nanolayers.

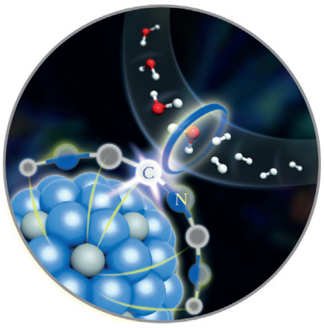

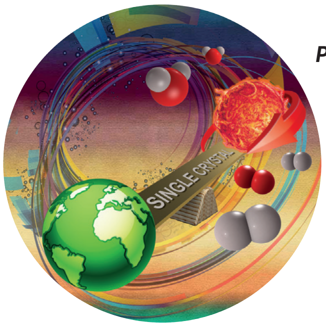

Photoelectrodes

T. Wang and J. Gong report recent research advances in using single-crystal semiconductors with narrow band gaps as photoelectrodes for solar water splitting in their Minireview on page 10718 ff.

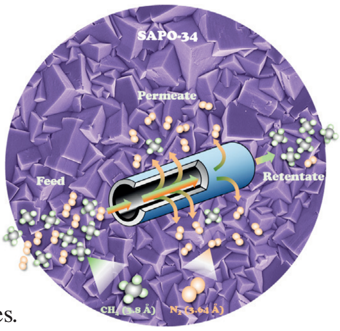

Membranes

In their Communication on page 10843 ff., S. Li, M. Yu, et al. present greatly improved zeolite membranes from high-aspect-ratio zeolite seeds that show high performance in separating N_2/CH_4 mixtures.

How to contact us:

Editorial Office:
E-mail: angewandte@wiley-vch.de
Fax: (+49) 6201–606-331
Telephone: (+49) 6201–606-315

Reprints, E-Prints, Posters, Calendars:
Carmen Leitner
E-mail: chem-reprints@wiley-vch.de
Fax: (+49) 6201–606-331
Telephone: (+49) 6201–606-327

Copyright Permission:
Bettina Loycke
E-mail: rights-and-licences@wiley-vch.de
Fax: (+49) 6201–606-332
Telephone: (+49) 6201–606-280

Online Open:
Margitta Schmitt
E-mail: angewandte@wiley-vch.de
Fax: (+49) 6201–606-331
Telephone: (+49) 6201–606-315

Subscriptions:
www.wileycustomerhelp.com
Fax: (+49) 6201–606-184
Telephone: 0800 1800536 (Germany only)
+44(0) 1865476721 (all other countries)

Advertising:
Marion Schulz
E-mail: mschulz@wiley-vch.de
Fax: (+49) 6201–606-550
Telephone: (+49) 6201–606-565

Courier Services:
Boschstrasse 12, 69469 Weinheim

Regular Mail:
Postfach 101161, 69451 Weinheim

Angewandte Chemie International Edition is a journal of the Gesellschaft Deutscher Chemiker (GDCh), the largest chemistry-related scientific society in continental Europe. Information on the various activities and services of the GDCh, for example, cheaper subscription to *Angewandte Chemie International Edition*, as well as applications for membership can be found at **www.gdch.de** or can be requested from GDCh, Postfach 900440, D-60444 Frankfurt am Main, Germany.

GDCh
GESELLSCHAFT
DEUTSCHER CHEMIKER

Editorial

S. Kitagawa* ———— **10686 – 10687**

Porous Materials and the Age of Gas

"... Materials that achieve mass storage and highly efficient separation of gases cannot be realized by simply improving conventional technology. The achievements in the field of metal–organic frameworks have rapidly and significantly advanced materials research that is vital to addressing energy and environmental issues..."
Read more in the Editorial by Susumu Kitagawa.

Service

Spotlight on Angewandte's Sister Journals **10706 – 10709**

Author Profile

Jose Luis Mascareñas ———— **10710**

"When I was eighteen I wanted to be an inventor. I advise my students to be open-minded and never stop questioning. ..."
This and more about Jose Luis Mascareñas can be found on page 10710.

News

European Inventor Award:
L. Leibler ———— **10711**

Praemium Academiae:
M. Hocek ———— **10711**

Gutenberg Research Award:
K. Kataoka ———— **10711**

L. Leibler

M. Hocek

K. Kataoka

Highlights

Epigenetics

D. Summerer* ________ **10714 – 10716**

N6-Methyladenine: A Potential Epigenetic Mark in Eukaryotic Genomes

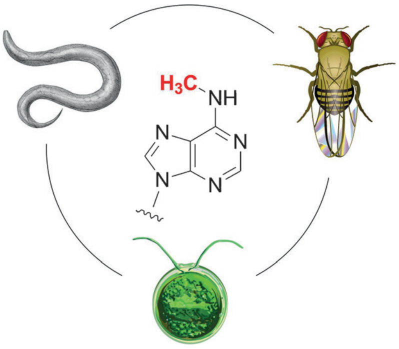

N6-methyladenine (6mA) is known to be an epigenetic mark in bacterial genomes. Three studies have now demonstrated the existence of significant levels of 6mA in the genomes of several phylogenetically distinct eukaryotes, along with findings that suggest that 6mA may act as a dynamic epigenetic mark in the regulation of eukaryotic gene expression.

Minireviews

Sustainable Chemistry

T. Wang, J. Gong* ________ **10718 – 10732**

Single-Crystal Semiconductors with Narrow Band Gaps for Solar Water Splitting

Inside Back Cover

With suitable band gaps and low bulk recombination, single-crystal semiconductors with narrow band gaps have shown excellent performance in solar water splitting. This Minireview describes recent research advances in using these semiconductors as efficient photoelectrodes, where surface protection, co-catalyst loading, surface energetics matching, and surface texturization are proposed as the most important approaches to realized high activity.

Reviews

Supported Graphene

A. Criado,* M. Melchionna, S. Marchesan, M. Prato* ________ **10734 – 10750**

The Covalent Functionalization of Graphene on Substrates

Covalent modification of graphene on substrates allows fine control of its chemical structure and opening of the bandgap for electronic applications. The graphene type and morphology, the nature of the substrate, and mechanical forces are key factors affecting reactivity. Analysis of these parameters and comparison of the different functionalization routes is essential to make an informed choice when working with functionalized graphene on a support.

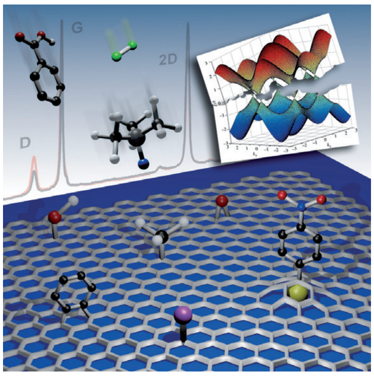

For the USA and Canada: ANGEWANDTE CHEMIE International Edition (ISSN 1433-7851) is published weekly by Wiley-VCH, PO Box 191161, 69451 Weinheim, Germany. US mailing agent: SPP, PO Box 437, Emigsville, PA 17318. Periodicals postage paid at Emigsville, PA. US POSTMASTER: send address changes to *Angewandte Chemie*, John Wiley & Sons Inc., C/O The Sheridan Press, PO Box 465, Hanover, PA 17331. Annual subscription price for institutions: US$ 11.738/10.206 (valid for print and electronic / print or electronic delivery); for individuals who are personal members of a national chemical society prices are available on request. Postage and handling charges included. All prices are subject to local VAT/sales tax.

Hydrogen-Evolution Reaction

Y. Liu, G. Yu, G.-D. Li, Y. Sun, T. Asefa,*
W. Chen,* X. Zou* ______ 10752 – 10757

Coupling Mo$_2$C with Nitrogen-Rich Nanocarbon Leads to Efficient Hydrogen-Evolution Electrocatalytic Sites

Frontispiece

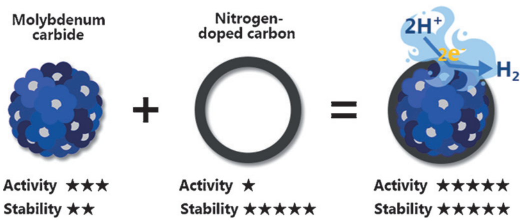

Hybrid catalyst: An efficient hybrid hydrogen-evolution electrocatalyst containing molybdenum carbide nanoparticles embedded in nitrogen-rich carbon nanolayers has been synthesized in one-step from inexpensive precursors. The synergistic effect between Mo$_2$C and N dopants was found to yield very active nonmetallic HER catalytic sites on the carbon nanolayers.

CO$_2$ Reduction

A. S. Varela, N. Ranjbar Sahraie,
J. Steinberg, W. Ju, H.-S. Oh,
P. Strasser* ______ 10758 – 10762

Metal-Doped Nitrogenated Carbon as an Efficient Catalyst for Direct CO$_2$ Electroreduction to CO and Hydrocarbons

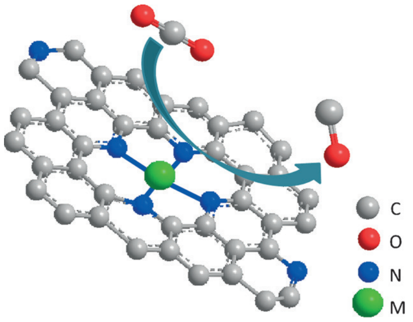

The kinetics, mechanism, and active sites of the CO$_2$ electroreduction reaction (CO2RR) to syngas and hydrocarbons on solid carbon-based catalysts doped with nitrogen, Fe, and/or Mn are explored. The solid powder catalysts are active and highly CO selective in CO2RR to CO/H$_2$ mixtures, outperforming a low-area polycrystalline gold benchmark.

Reaction Intermediates

Y. Yamanaka, Y. Kato, K. Hashimoto,
K. Iida, K. Nagasawa, H. Nakayama,
N. Dohmae, K. Noguchi, T. Noguchi,
M. Yohda, M. Odaka* ___ 10763 – 10767

Time-Resolved Crystallography of the Reaction Intermediate of Nitrile Hydratase: Revealing a Role for the Cysteinesulfenic Acid Ligand as a Catalytic Nucleophile

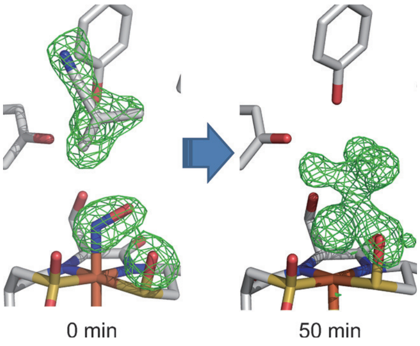

Visualizing enzyme reactions: The catalytic reaction of nitrile hydratase is monitored by time-resolved crystallography (see picture; C gray, N blue, O red, S yellow, Fe orange). Upon light-induced release of NO, the substrate observed in the pocket turned to bind to the Fe ion to form a cyclic reaction intermediate. The structure of the intermediate shows that the coordinated substrate is attacked by the sulfenate ligand.

Organoborane Macrocycles

P. Chen, X. Yin, N. Baser-Kirazli,
F. Jäkle* ______ 10768 – 10772

Versatile Design Principles for Facile Access to Unstrained Conjugated Organoborane Macrocycles

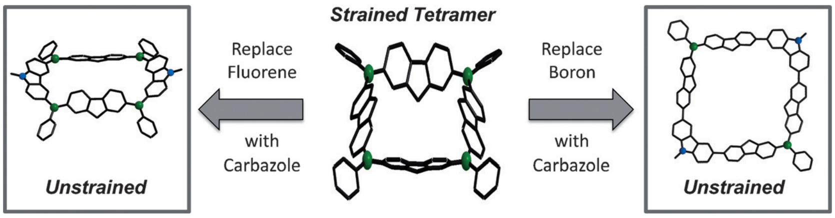

Changing shapes: Guided by theoretical calculations, the conjugated fluorene bridges or the borane moieties in a strained tetramer are partially replaced with carbazoles, resulting in hybrid macrocycles with new shapes and sizes. These macrocycles are ambipolar and show interesting emission characteristics and anion response, including anion-triggered geometry changes.

Fluorination

Y. Zeng, G. Li, J. Hu* ____ **10773 – 10777**

Diphenyliodonium-Catalyzed Fluorination of Arynes: Synthesis of *ortho*-Fluoroiodoarenes

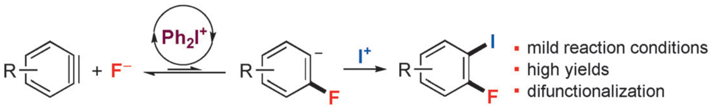

iCatalysis: A diphenyliodonium salt proved to be a privileged catalyst for nucleophilic fluorination of arynes using CsF as a fluorine source. A subsequent electrophilic iodination with C_4F_9I was also found to be crucial to ensure the efficient fluorination step.

Imaging Agents

S. R. Banerjee,* E. J. Ngen, M. W. Rotz, S. Kakkad, A. Lisok, R. Pracitto, M. Pullambhatla, Z. Chen, T. Shah, D. Artemov, T. J. Meade, Z. M. Bhujwalla, M. G. Pomper ____ **10778 – 10782**

Synthesis and Evaluation of Gd^{III}-Based Magnetic Resonance Contrast Agents for Molecular Imaging of Prostate-Specific Membrane Antigen

Good visibility: The relaxometric properties of a rationally designed high-affinity trimeric Gd^{III}-based contrast agent were evaluated in prostate cancer cells and in an in vivo experimental model (see picture; ΔR_1 measures contrast enhancement from 0% (blue) to 50% (red)) to demonstrate the feasibility of magnetic resonance molecular imaging of cells and tissues expressing prostate-specific membrane antigen (PSMA).

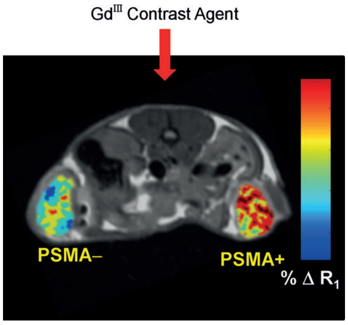

Magnetic Anisotropy

O. A. Blackburn, N. F. Chilton, K. Keller, C. E. Tait, W. K. Myers, E. J. L. McInnes, A. M. Kenwright, P. D. Beer, C. R. Timmel, S. Faulkner* ____ **10783 – 10786**

Spectroscopic and Crystal Field Consequences of Fluoride Binding by [Yb·DTMA]$^{3+}$ in Aqueous Solution

F makes the difference: [Yb·DTMA·OH$_2$]$^{3+}$ and [Yb·DTMA·F]$^{2+}$ are in slow exchange on the NMR timescale ($k_{ex} < 2000\ s^{-1}$), and profound differences are observed in the NMR and EPR spectra of these species. This behavior is explained by changes in the magnetic anisotropy of the Yb^{III} ground state from easy-axis to easy-plane type (see picture).

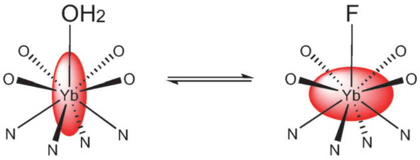

Lithium-Ion Batteries

F. F. Wu, S. L. Xiong,* Y. T. Qian, S. H. Yu* ____ **10787 – 10791**

Hydrothermal Synthesis of Unique Hollow Hexagonal Prismatic Pencils of $Co_3V_2O_8 \cdot n H_2O$: A New Anode Material for Lithium-Ion Batteries

Hydrothermal synthesis: A new phase of $Co_3V_2O_8 \cdot n H_2O$ hollow hexagonal prismatic pencils has been synthesized hydrothermally by varying the amount of NaOH in the reaction in the presence of NH_4^+ ions and absence of any template or surfactant (see picture). The excellent electrochemical activity results from the unique structure of $Co_3V_2O_8 \cdot n H_2O$ and probably from synergetic effects of different metal ions.

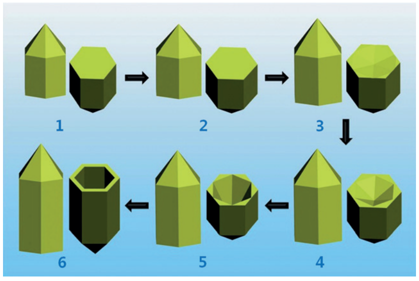

Fused-Ring Systems

A. K. Dutta, A. Linden, L. Zoppi,
K. K. Baldridge,*
J. S. Siegel* ______ **10792 – 10796**

Extended Corannulenes: Aromatic Bowl/Sheet Hybridization

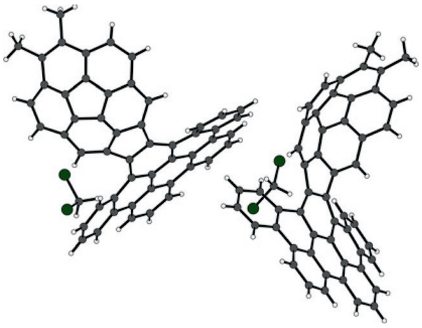

Caught and bowled: Photophysical and voltammetric studies together with high-level computations have been carried out on polynuclear aromatic hydrocarbons with distinct planar and bowl regions. A buckybowl–graphene hybrid was synthesized (see X-ray structure) as a model by activation of a C(Ar)$-$F bond. Curvature and extended π-effects were found to affect the properties of such materials.

Reaction Yields

F. S. Emami, A. Vahid, E. K. Wylie,
S. Szymkuć, P. Dittwald, K. Molga,
B. A. Grzybowski* ______ **10797 – 10801**

A Priori Estimation of Organic Reaction Yields

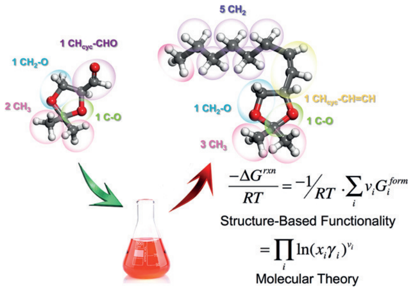

Getting to grips with yields: A thermodynamically guided calculation of free energies of substrate and product molecules allows the a priori estimation of the yields of organic reactions to be made. The model is first trained on a diverse set of reactions and reaction yields, and can then estimate the yields of other reactions with the accuracy of ±15%.

Carbon Nanotubes

Y. Nakanishi, H. Omachi, N. A. Fokina,
P. R. Schreiner, R. Kitaura, J. E. P. Dahl,
R. M. K. Carlson,
H. Shinohara* ______ **10802 – 10806**

Template Synthesis of Linear-Chain Nanodiamonds Inside Carbon Nanotubes from Bridgehead-Halogenated Diamantane Precursors

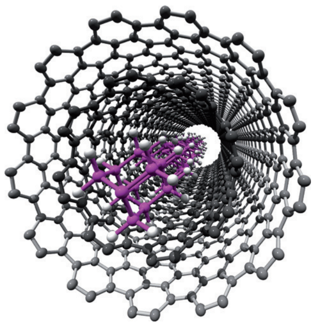

Long diamonds: A simple method for the synthesis of linear-chain diamond-like nanomaterials, so-called diamantane polymers, is described. This synthetic approach is primarily based on a template reaction of dihalogen-substituted diamantane precursors in the hollow cavities of carbon nanotubes. The present strategy may be used for the design and synthesis of other one-dimensional nanomaterials.

Front Cover

Foldamers

A. Altmayer-Henzien, V. Declerck,
J. Farjon, D. Merlet, R. Guillot,
D. J. Aitken* ______ **10807 – 10810**

Fine Tuning of β-Peptide Foldamers: a Single Atom Replacement Holds Back the Switch from an 8-Helix to a 12-Helix

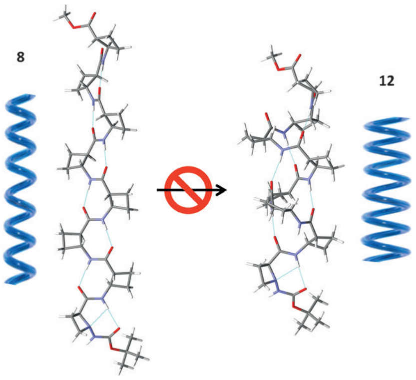

Keep it long and slim: Although a stable 12-helix conformer is available to oligo-β-peptides constructed from cyclic monomers, when an aza-adapted N terminus is incorporated, the resulting hydrazino turn feature leads the foldamer to preferentially adopt a more slimline 8-helix. This effect illustrates atomic-level programmable design for the fine tuning of peptide foldamer architectures.

Hybrid Materials

O. Riou, B. Lonetti,* R. P. Tan, J. Harmel,
K. Soulantica, P. Davidson,
A.-F. Mingotaud, M. Respaud,
B. Chaudret, M. Mauzac _ **10811 – 10815**

Room-Temperature, Strain-Tunable Orientation of Magnetization in a Hybrid Ferromagnetic Co Nanorod–Liquid Crystalline Elastomer Nanocomposite

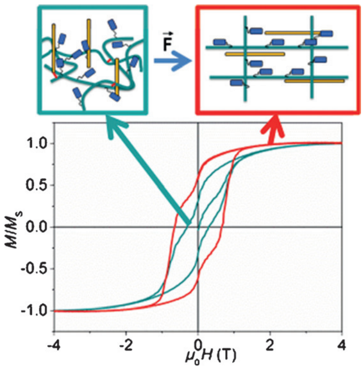

A highly anisotropic magnetic material with a strain tunable orientation of the magnetic direction was synthesized. In this material Co nanorods are aligned through a cross-linking process performed in the presence of an external magnetic field. The nanorod alignment can be switched at will at room temperature.

Lipid Bilayers

S. H. R. Shin, H. Y. Lee,
K. J. M. Bishop* ________ **10816 – 10820**

Amphiphilic Nanoparticles Control the Growth and Stability of Lipid Bilayers with Open Edges

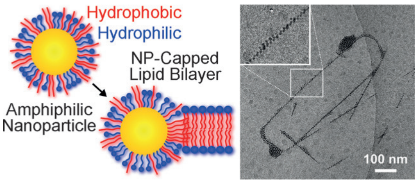

Nanoparticle surfactants that present mixtures of hydrophilic and hydrophobic ligands on their surface bind selectively at the open edge of bilayer membranes to stabilize amphiphile assemblies and control their growth. This general mechanism can be applied to inhibit formation of undesired assemblies such as cholesterol gallstones and to direct the growth of lipid nanostructures.

Imaging Probes

L. Li, C.-W. Zhang, J. Ge, L. Qian,
B.-H. Chai, Q. Zhu, J.-S. Lee, K.-L. Lim,
S. Q. Yao* __________ **10821 – 10825**

A Small-Molecule Probe for Selective Profiling and Imaging of Monoamine Oxidase B Activities in Models of Parkinson's Disease

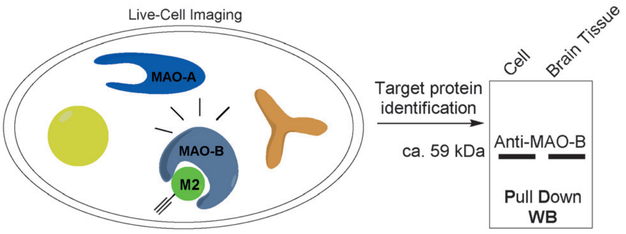

Seeing is believing: A dual-purpose small-molecule activity-based probe (**M2**) was developed for imaging the activity of monoamine oxidase B (MAO-B). In situ proteome profiling and live-cell bioimaging of endogenous MAO-B activities from a variety of biological samples, including Parkinson's disease models, can thus be carried out simultaneously.

Biomolecular Self-Assembly

Y. Zhang, R. M. Malamakal,
D. M. Chenoweth* _____ **10826 – 10832**

A Single Stereodynamic Center Modulates the Rate of Self-Assembly in a Biomolecular System

The influence of asymmetric carbon on biopolymer folding is of great importance as a general pre-organizing element in life processes. It is shown that a single C to N mutation in a collagen model peptide leads to a higher order structure with similar thermal unfolding but drastically different kinetic refolding behavior.

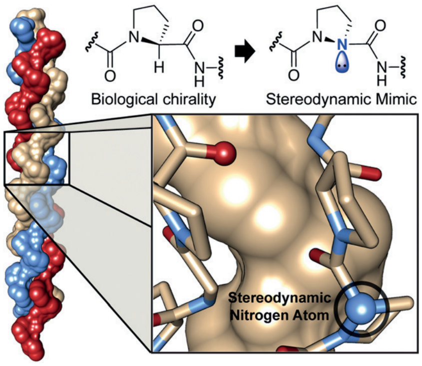

You'd better shape up: Two new polymorphs of the thyroid hormone thyroxine were characterized and it was found that polymorphism has a significant effect on the solubility and stability of this clinically useful compound. The conformational changes alter the electronic properties of the iodine atoms and the reactivity of the C–I bonds, which could have a significant effect on the hormone activity.

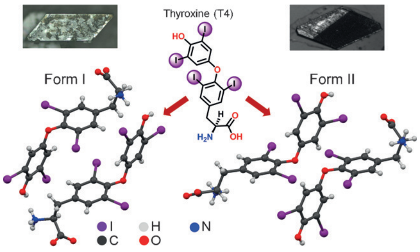

Polymorphism

S. Mondal, G. Mugesh* — **10833 – 10837**

Structure Elucidation and Characterization of Different Thyroxine Polymorphs

---

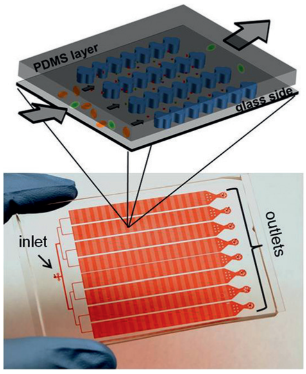

Stick with this one: When cancer cells were driven by hydrodynamic forces to flow through microchannels coated with basement membrane extract, highly adhesive cells were captured by the microchannels, and less adhesive cells were collected from the outlets (see picture). The less adhesive phenotype of two cancer cell lines was found to have a higher percentage of cancer stem cells, higher motility, and higher resistance to chemotherapeutic drugs.

Microfluidics

Y. Zhang, M. Wu, X. Han, P. Wang,*
L. Qin* ———— **10838 – 10842**

High-Throughput, Label-Free Isolation of Cancer Stem Cells on the Basis of Cell Adhesion Capacity

---

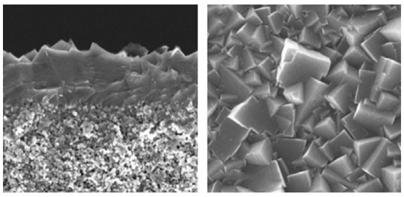

Slice-shaped zeolites: Thin SAPO-34 membranes of high quality were grown by using high-aspect-ratio SAPO-34 crystal seeds (see picture). A simultaneous increase in the N_2 permeance and N_2/CH_4 separation selectivity of the membranes was achieved. Incorporation of more Si into the crystal structure of these thin membranes resulted in a significantly increased N_2 permeance, while the N_2/CH_4 selectivity was maintained.

Membranes

Y. Huang, L. Wang, Z. Song, S. Li,*
M. Yu* ———— **10843 – 10847**

Growth of High-Quality, Thickness-Reduced Zeolite Membranes towards N_2/CH_4 Separation Using High-Aspect-Ratio Seeds

Back Cover

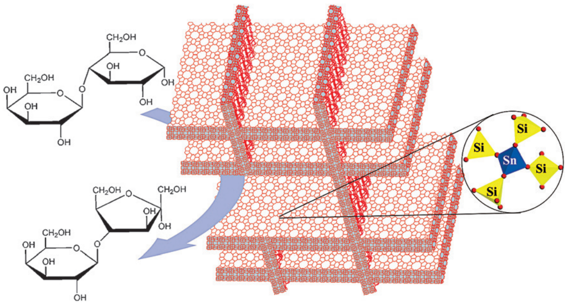

The adventures of thin tin: Sn is introduced in the framework of single-unit-cell (2 nm thick) zeolite MFI lamellae, which are intergrown in a self-pillared arrangement to obtain a hierarchical micro/mesoporous Lewis acid catalyst. Its conversion and selectivity are better than those of other micro- and mesoporous Sn-containing catalysts for isomerization of mono- and disacharides.

Zeolite Catalysts

VIP

L. Ren, Q. Guo, P. Kumar, M. Orazov,
D. Xu, S. M. Alhassan, K. A. Mkhoyan,
M. E. Davis,
M. Tsapatsis* ———— **10848 – 10851**

Self-Pillared, Single-Unit-Cell Sn-MFI Zeolite Nanosheets and Their Use for Glucose and Lactose Isomerization

Protein Profiling

D. Abegg, R. Frei, L. Cerato,
D. Prasad Hari, C. Wang, J. Waser,
A. Adibekian* ———— **10852 – 10857**

Proteome-Wide Profiling of Targets of Cysteine reactive Small Molecules by Using Ethynyl Benziodoxolone Reagents

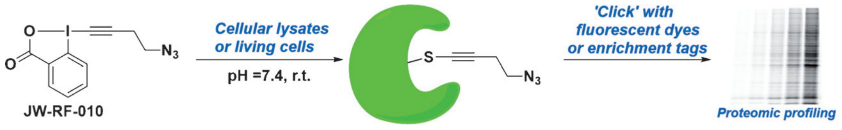

Good grip: Alkynyl benziodoxolones (EBX reagents) swiftly and highly selectively react with cysteine residues in cellular lysates and in living cells under physiological conditions. A “clickable” EBX probe allowed identification of the biological targets of natural product curcumin. This new method for cysteine labeling is particularly useful for various chemical proteomics applications.

EPR Spectroscopy

A. Fernandez, E. Moreno Pineda,
C. A. Muryn, S. Sproules, F. Moro,
G. A. Timco, E. J. L. McInnes,
R. E. P. Winpenny* ———— **10858 – 10861**

g-Engineering in Hybrid Rotaxanes To Create AB and AB_2 Electron Spin Systems: EPR Spectroscopic Studies of Weak Interactions between Dissimilar Electron Spin Qubits

Spin control: Hybrid [2]rotaxanes and pseudorotaxanes, such as $\{[Cu(hfac)_2][PyCH_2NH_2CH_2CH_2Ph][Cr_7Ni(\mu\text{-}F)_8(O_2CtBu)_{16}]\}$ (see picture; Hhfac = 1,1,1,6,6,6-hexafluoroacetylacetone), are reported where the magnetic interaction between dissimilar spins is controlled to create AB and AB_2 electron spin systems, allowing independent control of weakly interacting $S = {}^1\!/_2$ centers. Atom colors: Cr = green, Ni = purple, Cu = dark blue, F = yellow, O = red, C = gray, N = pale blue.

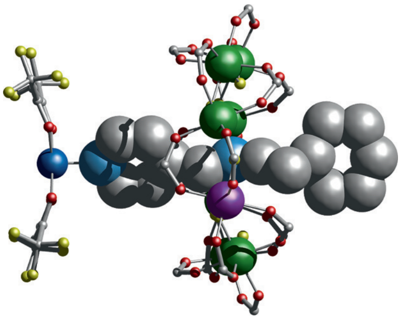

Light-Emitting Diodes

H.-D. Nguyen, C. C. Lin,
R. S. Liu* ———— **10862 – 10866**

Waterproof Alkyl Phosphate Coated Fluoride Phosphors for Optoelectronic Materials

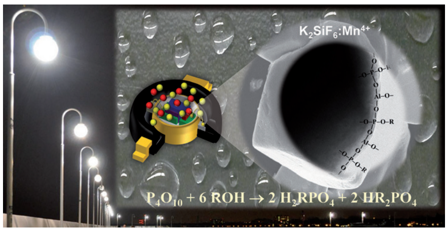

The moisture instability of fluoride phosphors has limited their application in optoelectronic devices. Their waterproof properties can be improved by a hydrophobic coating layer, such as an alkyl phosphate. The luminous efficacy of warm white-light-emitting diodes (WLEDs) based on such coated phosphors is remarkably stable even under high-humidity and high-temperature conditions.

Protein Folding

E. Di Silvio, M. Brunori,
S. Gianni* ———— **10867 – 10869**

Frustration Sculpts the Early Stages of Protein Folding

Diverging demands between folding and function cause a pattern of local frustration in proteins. By comparing the folding of proteins sharing nearly identical sequence and structure but displaying different frustration, it may be observed how frustration sculpts the early stages of folding whereas the late stages are more robust and biased by native topology.

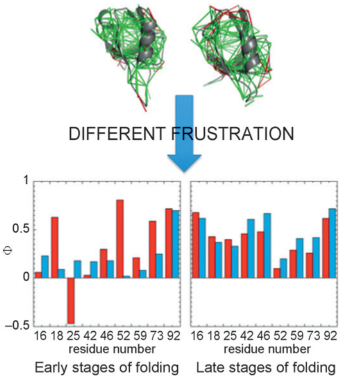

Perovskites

Y. Akizuki, I. Yamada,* K. Fujita,* K. Taga,
T. Kawakami, M. Mizumaki,
K. Tanaka **10870 – 10874**

Rattling in the Quadruple Perovskite $CuCu_3V_4O_{12}$

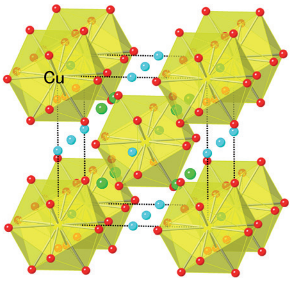

Oversize me: $CuCu_3V_4O_{12}$ is synthesized using a high-pressure technique. This compound adopts the cubic *A*-site ordered perovskite-type structure (space group $Im\bar{3}$) with a valence distribution of $Cu^{2+}Cu^{2+}_3V^{4+}_4O_{12}$. It has oversized icosahedral cages in which loosely bound *A*-site Cu^{2+} ions rattle with a characteristic temperature (Einstein temperature) of $\Theta_E \approx 55$ K. This is the first demonstration of rattling in perovskites.

Total Synthesis

J. H. Kim, S. Lee, S. Kim* **10875 – 10878**

Biomimetic Total Synthesis of (−)-Penibruguieramine A Using Memory of Chirality and Dynamic Kinetic Resolution

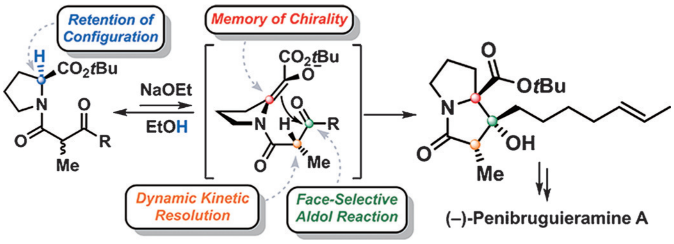

Chiral survival: The fully stereocontrolled total synthesis of (−)-penibruguieramine A is described. The principles of "memory of chirality" (MOC) and "dynamic kinetic resolution" (DKR) are applied to the biomimetic aldol reaction for the asymmetric synthesis, using proline as the only chiral source.

Biodegradable Polymers

Q. Zhang, Z. Hou, B. Louage, D. Zhou,
N. Vanparijs, B. G. De Geest,*
R. Hoogenboom* **10879 – 10883**

Acid-Labile Thermoresponsive Copolymers That Combine Fast pH-Triggered Hydrolysis and High Stability under Neutral Conditions

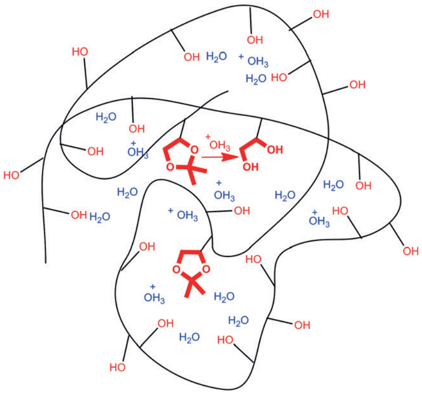

Breaking the rules: Thermoresponsive polymers with both dimethyldioxolane and hydroxyethyl side chains were hydrolyzed rapidly under slightly acidic conditions while being stable at pH 7.4 or during storage: important properties for biomedical applications. Thus, hydrolysis of the acid-labile cyclic-acetal groups was accelerated by the presence of hydroxy groups, which led to enhanced hydration of the collapsed copolymer globules (see picture).

Cross-Coupling

M. U. Luescher,
J. W. Bode* **10884 – 10888**

Catalytic Synthesis of N-Unprotected Piperazines, Morpholines, and Thiomorpholines from Aldehydes and SnAP Reagents

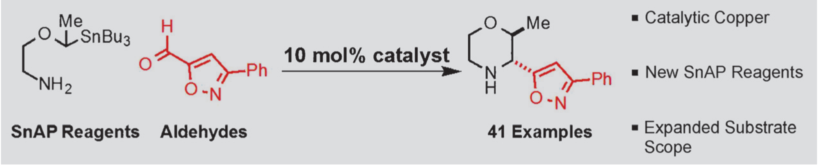

SnAPcat! The identification of new ligands and reaction conditions provides a robust catalytic method for the synthesis of N-unprotected heterocycles using SnAP reagents. This catalytic variant expands the substrate scope to include previously inaccessible piperazines, morpholines, and thiomorpholines and establishes the basis for a catalytic enantioselective process through the use of chiral ligands.

Metal–Organic Frameworks

J. Yang, F. Zhang, H. Lu, X. Hong, H. Jiang, Y. Wu,* Y. Li* **10889 – 10893**

Hollow Zn/Co ZIF Particles Derived from Core–Shell ZIF-67@ZIF-8 as Selective Catalyst for the Semi-Hydrogenation of Acetylene

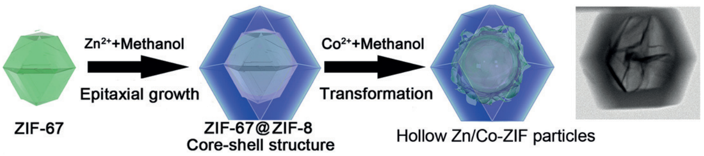

A mild phase transformation of ZIF-67@ZIF-8 core–shell structures is achieved under solvothermal conditions to generate unique hollow Zn/Co ZIF particles, which were used to generate Pd@MOF yolk-shell composites. They exhibit enhanced gas storage and high catalytic activity and selectivity in the semi-hydrogenation of acetylene.

Glycosylations

J.-S. Huang, W. Huang, X. Meng, X. Wang, P.-C. Gao, J.-S. Yang* **10894 – 10898**

Stereoselective Synthesis of α-3-Deoxy-D-*manno*-oct-2-ulosonic Acid (α-Kdo) Glycosides Using 5,7-*O*-Di-*tert*-butylsilylene-Protected Kdo Ethyl Thioglycoside Donors

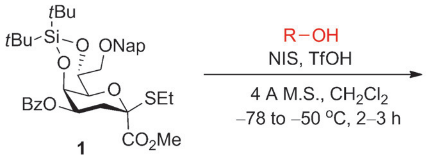

A Kdo K.O.: The title compound is a common structural constituent of polysaccharides present in bacteria. An approach to stereospecific synthesis of α-Kdo glycosides was developed by using 5,7-*O*-di-*tert*-butylsilylene-protected Kdo ethyl thioglycoside donors (**1**). Various α-Kdo glycosidic linkages were constructed in good to excellent chemical yields with complete α-selectivity (**2**). M.S. = molecular sieves, NIS = *N*-iodosuccinimide, Tf = trifluoromethanesulfonyl.

Biocatalysis

E. Busto,* R. C. Simon, W. Kroutil* **10899 – 10902**

Vinylation of Unprotected Phenols Using a Biocatalytic System

Inside Cover

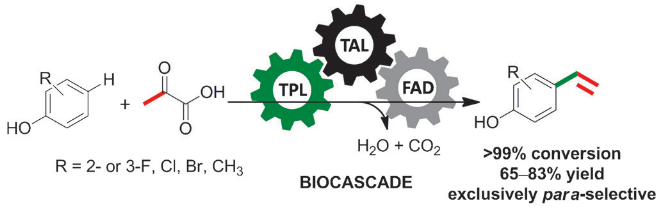

Make it simple! A biocatalytic system for the selective *para* vinylation of substituted phenols provides the desired products with > 99% conversion in water. An efficient metal-free method for the atom-economic preparation of *para*-vinylphenols under mild reaction conditions has thus been developed.

Cyclizations

C. Yu, B. Chen, T. Zhou, Q. Tian, G. Zhang* **10903 – 10907**

Gold(I)-Catalyzed Tandem Transformation with Diynes: Rapid Access to Linear Cyclopentenone-Fused Polycyclic Molecules

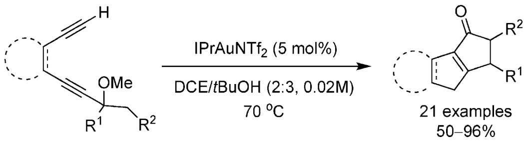

Linear cycles: An efficient and convenient synthesis of the title compounds has been achieved through a gold(I)-catalyzed transformation of diynes. A novel mechanism involving gold vinylidene formation, methoxy group migration, and a Nazarov-type cyclization is postulated. DCE = 1,2-dichloroethane, IPr = 1,3-bis-(diisopropylphenyl)imidazol-2-ylidene, Tf = trifluoromethanesulfonyl.

Expanded Porphyrins

Y. Tanaka, T. Yoneda, K. Furukawa,*
T. Koide, H. Mori, T. Tanaka,
H. Shinokubo, A. Osuka* 10908 – 10911

A Stable Organic π-Radical of a Zinc(II)–Copper(I)–Zinc(II) Complex of Decaphyrin

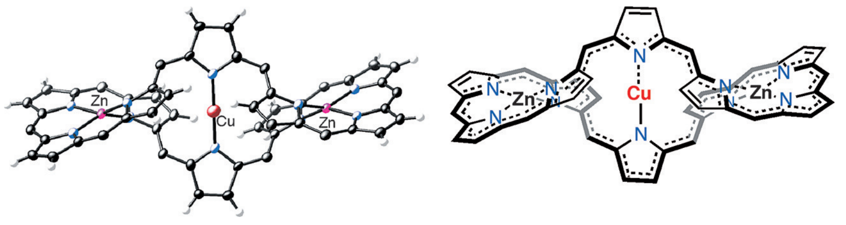

Radical racetrack: Cu^{II} metalation of a [46]decaphyrin bis(Zn^{II}) complex gave a Zn^{II}-Cu^{I}-Zn^{II} heterotrimetal complex of decaphyrin consisting of a central Cu^{I} ion and a monoanionic 45π radical of decaphyrin. Despite the radical nature, the complex is fairly stable under ambient conditions. This stability is probably due to the effective delocalization of an unpaired electron over the whole π-conjugation network of the decaphyrin.

Synthetic Methods

H. Yu, G. Zhang,
H. Huang* 10912 – 10916

Palladium-Catalyzed Dearomative Cyclocarbonylation by C—N Bond Activation

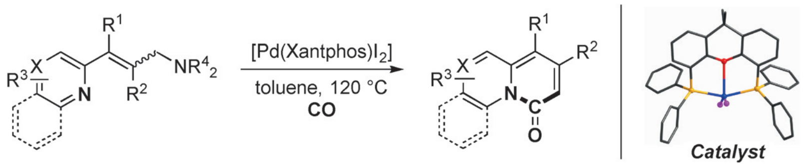

Dearomatization: A highly efficient dearomative cyclocarbonylation reaction proceeds by palladium-catalyzed C—N bond activation, dearomatization, CO insertion, and a Heck reaction. This transformation represents the first general catalytic method for the synthesis of valuable bioactive quinolizinones.

Asymmetric Catalysis

J. Liu, Y. Tian, J. Shi, S. Zhang,
Q. Cai* 10917 – 10920

An Enantioselective Synthesis of Spirobilactams through Copper-Catalyzed Intramolecular Double N-Arylation and Phase Separation

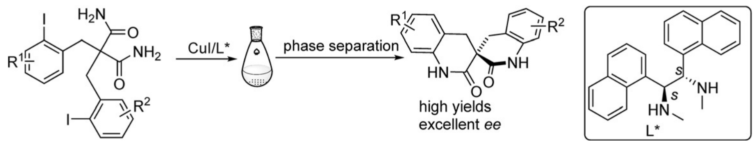

Spirocyclic structures are versatile building blocks for functional chiral molecules. A copper-catalyzed double N-arylation was developed for the enantioselective synthesis of chiral spirobilactams. Enantioenriched spirobilactams were obtained with excellent *ee* values through precipitation of the racemate and simple solid–solution phase separation.

Cluster Compounds

V. Cîrcu,* Y. Molard,* M. Amela-Cortes,
A. Bentaleb, P. Barois, V. Dorcet,
S. Cordier* 10921 – 10925

From Mesomorphic Phosphine Oxide to Clustomesogens Containing Molybdenum and Tungsten Octahedral Cluster Cores

Clustomesogens are metal atom clusters containing liquid-crystalline materials. They have been obtained by grafting neutral cyanobiphenyl- or cholesteryl-containing tailor-made dendritic mesomorphic triphenylphosphine oxide ligands on luminescent $(M_6Cl^i_8)^{4+}$ octahedral cluster cores (M = Mo, W).

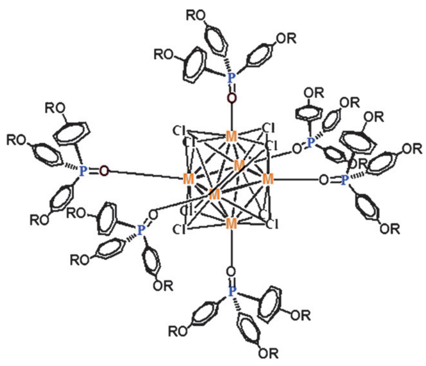

Heterocycle Synthesis

S. U. Dighe, S. Mukhopadhyay, S. Kolle, S. Kanojiya, S. Batra* ____ **10926 – 10930**

Synthesis of 3,4,5-Trisubstituted Isoxazoles from Morita–Baylis–Hillman Acetates by an $NaNO_2/I_2$-Mediated Domino Reaction

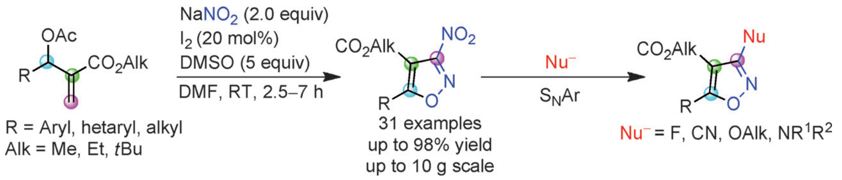

An efficient synthesis of highly substituted isoxazoles from the reaction of allyl acetates with $NaNO_2$ by using I_2 under oxidative conditions is demonstrated. The reactions proceed through an I_2-assisted activation of the C–H bond α to the nitro group, nucleophilic addition, and subsequent [3+2] cycloaddition. DMF = *N*,*N*-dimethylformamide, DMSO = dimethylsulfoxide.

Peptide Macrocyclization

Y. Wang, D. H.-C. Chou* _ **10931 – 10934**

A Thiol–Ene Coupling Approach to Native Peptide Stapling and Macrocyclization

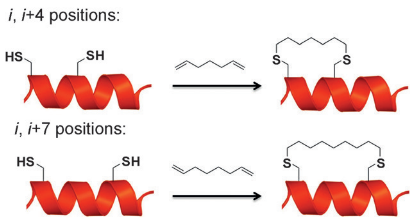

The selective modification of cysteine residues in native, unprotected peptides with a variety of stapling modifications for helix stabilization or general macrocyclization is achieved by a new peptide stapling and macrocyclization method. This method uses thiol–ene reactions between two cysteine residues and a diene and gives high yields.

Carbohydrates

A. Nakagawa, M. Tanaka, S. Hanamura, D. Takahashi,* K. Toshima* ____ **10935 – 10939**

Regioselective and 1,2-*cis*-α-Stereoselective Glycosylation Utilizing Glycosyl-Acceptor-Derived Boronic Ester Catalyst

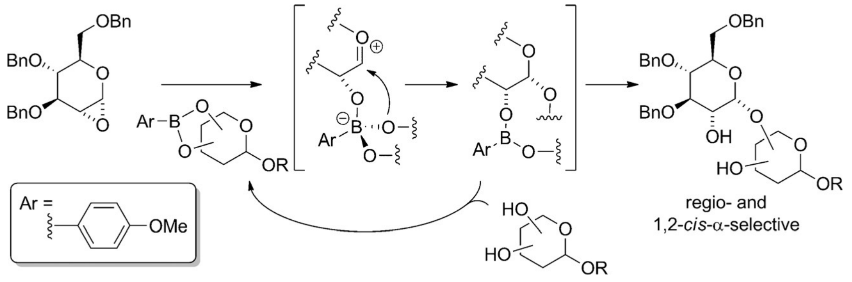

Donors and acceptors: The title reaction of 1α,2α-anhydro glycosyl donors and diol glycosyl acceptors proceeded smoothly to give the corresponding 1,2-*cis*-α-glycosides with high stereo- and regioselectivities. The glycosylation method was successfully applied to the synthesis of an isoflavone glycoside.

Natural Products

J. Ouyang, R. Yan, X. Mi, R. Hong* ____ **10940 – 10943**

Enantioselective Total Synthesis of (−)-Hosieine A

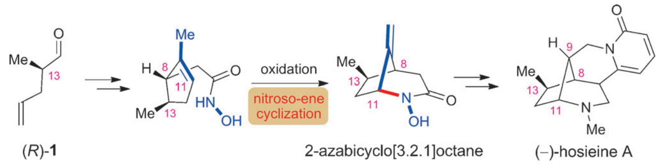

An unprecedented nitroso-ene cyclization to construct the 2-azabicyclo[3.2.1]octane ring system was developed during the first total synthesis of (−)-Hosieine A, a novel Lupin alkaloid possessing high affinity towards the α4β2 receptor with nanomolar level potency. Noteworthy transformations are the phosphine-enabled stereoselective bromohydrination and facile radical debromination initiated by Et_3B/air.

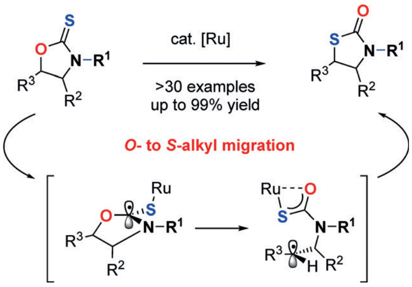

A radical step in a new direction: A practical ruthenium-catalyzed *O*- to *S*-alkyl migration affords structurally diverse thiooxazolidinones in excellent yields. Experimental and computational studies suggest a pseudoreversible radical pathway drawing mechanistic parallels to the classic Barton–McCombie reaction.

Pseudoreversible Reactions

W. Mahy, P. Plucinski, J. Jover,
C. G. Frost* ________ **10944 – 10948**

Ruthenium-Catalyzed *O*- to *S*-Alkyl Migration: A Pseudoreversible Barton–McCombie Pathway

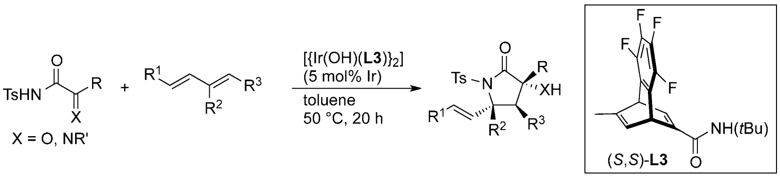

[3+2] annulation: The asymmetric [3+2] annulation of α-oxo- and α-iminocarboxamides with 1,3-dienes catalyzed by hydroxoiridium/chiral diene complexes was achieved. The reaction gives the corresponding γ-lactams in high yields with high enantioselectivity.

Asymmetric Annulation

M. Hatano,
T. Nishimura* ________ **10949 – 10952**

Hydroxoiridium/Chiral Diene Complexes as Effective Catalysts for Asymmetric Annulation of α-Oxo- and Iminocarboxamides with 1,3-Dienes

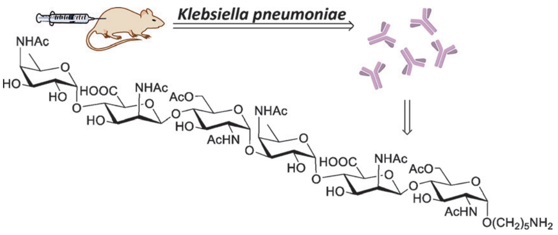

Hitting the sweet spot: All *Enterobacteriaceae* express the polysaccharide enterobacterial common antigen (ECA), which is an attractive target for the development of universally acting immunotherapies. ECA-derived oligosaccharides were chemically synthesized and used to uncover immunodominant epitopes and develop a monoclonal antibody showing broad recognition of *Enterobacteriaceae*.

Oligosaccharides

L. Liu, J. Zha, A. DiGiandomenico,
D. McAllister, C. K. Stover, Q. Wang,*
G.-J. Boons* ________ **10953 – 10957**

Synthetic Enterobacterial Common Antigen (ECA) for the Development of a Universal Immunotherapy for Drug-Resistant *Enterobacteriaceae*

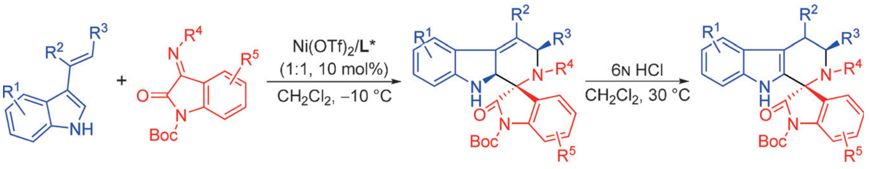

An asymmetric aza-Diels–Alder reaction of 3-vinylindoles with isatin-derived ketimines leads to spiroindolone derivatives with high regio-, diastereo-, and enantioselectivity and also provides facile access to the valuable antimalarial drug NITD609. The stereoselectivity is thought to arise from π–π interactions between the two reactants and the chiral *N*,*N*′-dioxide ligand.

Aza-Diels–Alder Reactions

H. F. Zheng, X. H. Liu,* C. R. Xu, Y. Xia,
L. L. Lin, X. M. Feng* ____ **10958 – 10962**

Regio- and Enantioselective Aza-Diels–Alder Reactions of 3-Vinylindoles: A Concise Synthesis of the Antimalarial Spiroindolone NITD609

Domino Reactions

K. Moriya, M. Simon, R. Mose,
K. Karaghiosoff,
P. Knochel* ______ **10963 – 10967**

Stereoselective Retentive Domino Transmetalations of Secondary Alkyllithium Compounds to Functionalized Secondary Alkylcopper Reagents

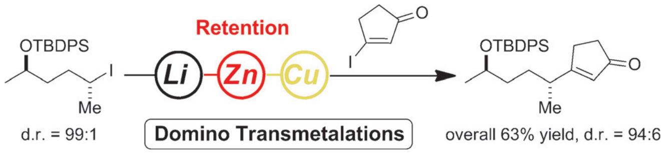

Configurationally retentive domino transmetalations of nonstabilized functionalized secondary alkyllithium compounds with $Me_3SiCH_2ZnBr{\cdot}LiBr$ and $CuBr{\cdot}2\,LiCl{\cdot}Me_2S$ allow the preparation of secondary alkylcopper compounds with retention of configuration (TBDPS = *tert*-butyldiphenylsilyl). Trapping with a range of electrophiles (acid chlorides, ethylene oxide, alkynyl esters, ketals, allylic chlorides) afford various open-chain acyclic products.

Pyrotechnics

J. J. Sabatini,* E.-C. Koch,* J. C. Poret,
J. D. Moretti,
S. M. Harbol ______ **10968 – 10970**

Chlorine-Free Red-Burning Pyrotechnics

Seeing red: The emission from $SrOH_{(g)}$ alone is responsible for the red color of a chlorine-free high-intensity flare based on magnesium, strontium nitrate, 5-amino-1*H*-tetrazole or hexamine, and Epon binder. The detrimental orange emission from $SrO_{(g)}$ could be successfully suppressed. The new formulations avoid any risk of forming carcinogenic polychlorinated aromatic compounds and will positively impact civilian and military pyrotechnics.

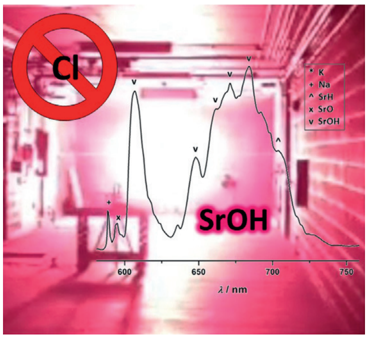

Molecular Evolution

F. Tolle, G. M. Brändle, D. Matzner,
G. Mayer* ______ **10971 – 10974**

A Versatile Approach Towards Nucleobase-Modified Aptamers

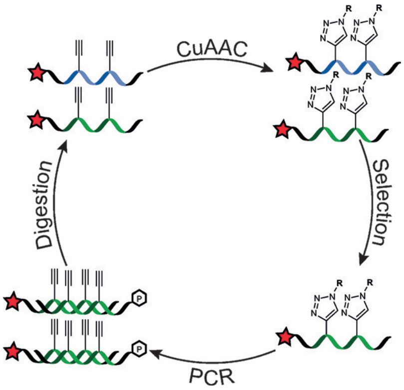

Click to select: A versatile method for modular expansion of the chemical space of nucleic acid libraries has been developed. This method enables the generation of nucleobase-modified aptamers with unprecedented recognition properties. In situ reintroduction of the modification after enzymatic replication gives broad access to many chemical modifications, thus enabling the application of in vitro selection approaches beyond what is feasible to date.

C–H Activation

J. H. Kim, T. Gensch, D. Zhao,
L. Stegemann, C. A. Strassert,*
F. Glorius* ______ **10975 – 10979**

Rh^{III}-Catalyzed C–H Activation with Pyridotriazoles: Direct Access to Fluorophores for Metal-Ion Detection

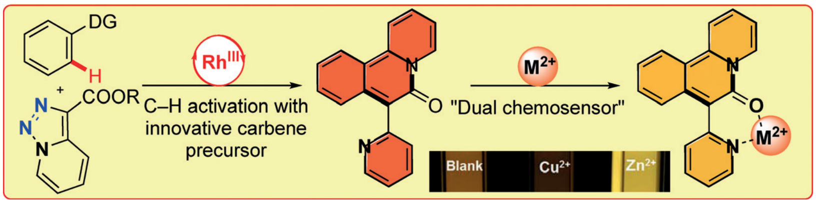

Form(ation) follows function: The first C–H bond activation with pyridotriazoles as a coupling partner is made possible by using a Rh^{III} catalyst. The pyridotriazoles serve as new carbene precursors in C–H activation allowing direct access to fluorescent scaffolds bearing a pyridine-type ligating group. These fluorophores can be applied as dual sensors for colorimetric sensing of Cu^{2+} ions and fluorescence sensing for Zn^{2+} ions.

The ties that bind: The highly repetitive structure of the collagen-binding protein decorin allowed the design of peptides representative of each of its two distinct sides. Strongly binding peptides (red) derived from the inner surface were conjugated to a dye or dimerized. These peptides bind to collagen and provide a biomimetic tool for tailoring biomaterials by controlling mechanical properties or compound diffusion in collagen gels.

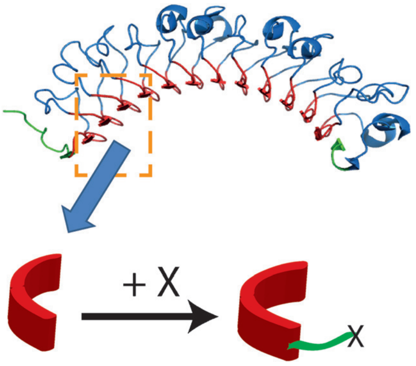

Peptides

S. Federico, B. F. Pierce, S. Piluso,
C. Wischke, A. Lendlein,
A. T. Neffe* ———— **10980 – 10984**

Design of Decorin-Based Peptides That Bind to Collagen I and their Potential as Adhesion Moieties in Biomaterials

---

Supporting information is available on www.angewandte.org (see article for access details).

A video clip is available as Supporting Information on www.angewandte.org (see article for access details).

This article is available online free of charge (Open Access).

This article is accompanied by a cover picture (front or back cover, and inside or outside).

The Very Important Papers, marked VIP, have been rated unanimously as very important by the referees.

The Hot Papers are articles that the Editors have chosen on the basis of the referee reports to be of particular importance for an intensely studied area of research.